

## Next generation modeling of microbial souring – Parameterization through genomic information



Yiwei Cheng<sup>a, \*</sup>, Christopher G. Hubbard<sup>b, 1</sup>, Liange Zheng<sup>b</sup>, Bhavna Arora<sup>b</sup>, Li Li<sup>c</sup>, Ulas Karaoz<sup>a</sup>, Jonathan Ajo-Franklin<sup>b</sup>, Nicholas J. Bouskill<sup>a</sup>

<sup>a</sup> Climate and Ecosystem Sciences Division, Lawrence Berkeley National Laboratory, 1 Cyclotron Rd, Berkeley, CA, USA

<sup>b</sup> Energy Geosciences Division, Lawrence Berkeley National Laboratory, 1 Cyclotron Rd Berkeley, CA, USA

<sup>c</sup> Department of Civil and Environmental Engineering, Pennsylvania State University, University Park, PA, USA

### ARTICLE INFO

#### Article history:

Received 31 December 2015

Received in revised form

16 June 2017

Accepted 22 June 2017

Available online 5 July 2017

#### Keywords:

Microbially mediated sulfate reduction

Oil reservoir

Genomics

Multiphase reactive transport model

### ABSTRACT

Biogenesis of hydrogen sulfide (H<sub>2</sub>S) (microbial souring) has detrimental impacts on oil production operations and can cause health and safety problems. Understanding the processes that control the rates and patterns of sulfate reduction is crucial in developing a predictive understanding of reservoir souring and associated mitigation processes. This work demonstrates an approach to utilize genomic information to constrain the biological parameters needed for modeling souring, providing a pathway for using microbial data derived from oil reservoir studies. Minimum generation times were calculated based on codon usage bias and optimal growth temperatures based on the frequency of amino acids. We show how these derived parameters can be used in a simplified multiphase reactive transport model by simulating the injection of cold (30 °C) seawater into a 70 °C reservoir, modeling the shift in sulfate reducing microorganisms (SRM) community composition, sulfate and sulfide concentrations through time and space. Finally, we explore the question of necessary model complexity by comparing results using different numbers of SRM. Simulations showed that the kinetics of a SRM community consisting of twenty-five SRM could be adequately represented by a reduced community consisting of nine SRM with parameter values derived from the mean and standard deviations of the original SRM.

Published by Elsevier Ltd. This is an open access article under the CC BY-NC-ND license (<http://creativecommons.org/licenses/by-nc-nd/4.0/>).

### 1. Introduction

Microorganisms play key roles in the life cycle of oil and gas formation, production, and bioremediation (Head et al., 2003, 2014; Youssef et al., 2007, 2009). During secondary oil production, seawater with typical sulfate concentration of ~28 mM, is often injected into oil reservoirs to maintain reservoir pressure and sweep out oil, potentially giving sulfate reducing microorganisms (SRM) the opportunity to couple the reduction of sulfate to bisulfide (HS<sup>-</sup>) with the biodegradation of crude oil derived organics, such as volatile fatty acids (VFAs), aromatics (e.g. toluene) and aliphatic hydrocarbons. The sulfide produced by this process (also known as microbial souring) presents significant corrosion (e.g. sulfide stress corrosion cracking of carbon steel infrastructure), health and safety, and economic problems to oil producers (Fuller

and Suruda, 2000; Vance and Thrasher, 2005; Semcrude, 2011). Understanding and preventing souring is therefore an ongoing priority for the industry.

Reservoir models are essential management tools used across the oil industry to understand and predict fluid flow in the subsurface during different stages of oil production. Increasingly, accurate representation of souring has become a priority (Haghshenas et al., 2012). This is not a trivial problem, as the process of water injection into an oil reservoir develops gradients in a range of important environmental characteristics, and these gradients vary in time and space as water injection continues. For example, the injection of relatively cold seawater into a hotter reservoir produces gradients in temperature, sulfate (due to high concentrations in the injected seawater), and electron donor (higher crude oil derived organics in the formation water than the injection water). All of these dynamic, intersecting gradients provide a wide range of potential ecological niches for different SRM, potentially leading to a diverse community which develops and changes through time and space as the changing environmental

\* Corresponding author.

E-mail address: [yiweicheng@lbl.gov](mailto:yiweicheng@lbl.gov) (Y. Cheng).

<sup>1</sup> Now at Water Research Institute, Cardiff University, Cardiff, Wales.

conditions imposed by water flooding preferentially select for certain SRM over others as demarcated by their physiological characteristics (or traits). Most modeling studies assumed that the kinetics of the diverse SRM can be effectively represented by a single set of kinetic parameters (e.g. maximum growth rate and half saturation constant for electron acceptors and donors). Models of experiments conducted under constant environmental conditions further assume the kinetic parameter values to be constant (e.g. constant maximum growth rate under isothermal conditions) (Cheng et al., 2016). Under this scheme, 'optimal' values of the kinetic parameters are systematically derived from calibrations that fit observed data. While computationally simple, such representations are far from reality. Microbial communities are typically diverse and their distributions stochastic. Within natural communities, organisms thrive by maximizing their fitness relative to their environmental conditions and other competitors. Community composition is therefore an emergent property that constantly evolves as communities self-organize in response to heterogeneous environmental conditions. When each organism maximizes its own growth, they collectively maximize the rate of a given process (e.g. sulfate reduction) under the prevailing environmental condition. It is therefore important for models to sufficiently capture the microbial complexity that can potentially emerge under these fluctuating conditions. Insufficient complexity runs the risk of diminishing the predictive power of a model as conditions and gradients evolve through time, whereas too much complexity increases computational demands and may be under-constrained by available data. To investigate this problem of complexity we take advantage of two rapidly developing fields: increased sophistication in modeling microbial processes, and the greater utilization of microbial genomics providing understanding of microbial function and diversity in the environment.

Microbial models that predict the structure and activity of the microbial community on the basis of physiological and ecological traits of different microbial guilds have increasingly gained traction as approaches for further understanding the response of a microbial community to perturbation (Le Roux et al., 2016) or to better represent microbial function in more established models (Follows et al., 2007). The increasing utilization of a trait-based approach lies in the advantages of reducing the complexity of the microbial community to several different functional guilds on the basis of traits related to substrate utilization, growth, carbon use efficiency and their response to environmental factors (e.g. temperature). Parameterizing different combinations of these traits can determine an individual organism's fundamental niche (Holt, 2009). The realized niche is then determined through competition with different modeled microbial guilds for common substrates (electron donors or acceptors). This reductionist approach can therefore discreetly reproduce the functional basis of a given microbial community without the computational intractability or ecological redundancy of representing all of the individual microorganisms.

Souring, as a microbially mediated process, is inherently amenable to representation through trait-based modeling. Both traditional isolation experiments and more recent genomic data provide abundant data on the physiological mechanisms that may be used to develop and parameterize trait-based models, including, for example, the range of electron donors the SRM may use (Muyzer and Stams, 2008). An important flexibility that may be represented by trait-based modeling frameworks is the competition by different functional guilds (e.g., denitrifiers and SRM) and linked processes (e.g., SRM and sulfide-oxidizing bacteria) that can lead to estimates of net production of sulfide, rather than bulk production rates. More recent proliferation of genomic data sets provides a wealth of potential data that can be used to identify specific traits of organisms. Significant advances in the identification and annotation of complex

(meta)genomic data sets (e.g., Wu et al., 2014) make the derivation and parameterization of key traits possible.

This work seeks to provide a way forward to more accurately represent oil reservoir microbial dynamics, thereby improving predictions of biogenic souring. To do this we first show how genomic information can be used to constrain the biological parameters needed for modeling souring, providing a pathway for using microbial data derived from oil reservoir studies. We then show how these derived parameters can be used in a simplified reactive transport simulation of seawater injection into a reservoir. Finally, we explore the question of necessary model complexity by comparing model results using different numbers of sulfate reducers.

## 2. Methods

### 2.1. Deriving model parameters from microbial datasets

Genomic data provides insights related to important traits that can be used to constrain the parameterization of the current generation of models. While there are multiple traits that can be derived from genomic data, optimal growth temperatures and minimum generation time have been shown to have good correlation to observational data. The generation time of individual groups within a guild is an important trait in the models, and can be estimated by examining the codon usage bias evident within highly expressed genes from individual genomes (Vieira-Silva and Rocha, 2010). Similarly, another important trait, the optimal growth temperature, is found in the preferential use of several amino acids, for which the corresponding signatures may also be discerned from the genomes (Zeldovich et al., 2007).

Minimum generation (doubling) times were predicted based on codon usage bias between all genes and in a set of highly expressed genes following the linear regression model from (Vieira-Silva and Rocha, 2010). We used ribosomal protein genes as the set of highly expressed genes. Genome sequences for twenty-five SRMs were downloaded from Genbank genomes (<ftp://ftp.ncbi.nih.gov/genomes/Bacteria/>) (Table 1). (Note: Only closed genomes were downloaded). Genes and their annotations were extracted from annotation files (.ppt files) and genes for ribosomal proteins were identified based on the annotation fields. Using the nucleotide sequences for the two set of genes, codon usage bias index,  $\Delta ENC'$ , was calculated using the following equation:

$$\Delta ENC' = \frac{ENC'_{all} - ENC'_{ribosomal\ protein\ genes}}{ENC'_{all}} \quad (1)$$

where  $ENC'$  is the effective number of codons given G + C composition (Novembre, 2002) and inputted to the above equation. Optimal growth temperature was calculated based on the frequency of amino acids IVYWREL in the proteome of the organism as in (Zeldovich et al., 2007). We conducted literature searches to acquire data on optimal growth temperature and minimum generation times for SRM. Data on eleven SRM were acquired for comparison against derived minimum generation times and optimal temperatures from genomic data. The SRM belong to the genus: *Archaeoglobus*, *Desulfatibacillum*, *Desulfococcus*, *Desulfosporosinus*, *Desulfovibrio*, *Desulfurococcus*, *Sulfurimonas*, *Thermodesulfobacterium* and *Thermodesulfobium* (see Table 2).

Kinetics of microbial growth under substrate limitation can be described by Monod equation (see Equation (3)). An important parameter in the Monod equation is the half saturation constant,  $K_s$ , which represents the affinity of the microbe for a particular substrate. Kinetic studies of dissimilatory sulfate reductions revealed a broad range of values of half saturation constants (sulfate),

**Table 1**  
Information on the 25 SRM from which we derived average minimum generation time and optimal growth temperature.

Genus	Species	Strain	NCBI Accession	#Ribosomal protein genes	#All genes	Predicted Avg. Min. Generation Time (hours)	Optimal T (°C)
<i>Archaeoglobus</i>	<i>fulgidus</i>	DSM4304	NC_000917	61	2346	1.63	83
<i>Archaeoglobus</i>	<i>profundus</i>	DSM5631	NC_013741	57	1761	0.80	95
<i>Archaeoglobus</i>	<i>sulfatcallidus</i>	PM70	NC_021169	63	2153	1.58	82
<i>Archaeoglobus</i>	<i>veneficus</i>	SNP6	NC_015320	58	2032	1.04	85
<i>Desulfatibacillum</i>	<i>alkenivorans</i>	AK	NC_011768	55	5197	7.92	24
<i>Desulfobacter</i>	<i>postgatei</i>	2ac9	NZ_CM001488	60	3353	7.41	28
<i>Desulfobulbus</i>	<i>propionicus</i>	DSM2032	NC_014972	50	3228	2.62	43
<i>Desulfococcus</i>	<i>oleovorans</i>	Hxd3	NC_009943	55	3210	12.02	30
<i>Desulfomicrobium</i>	<i>baculatum</i>	DSM4028	NC_013173	53	3382	3.17	39
<i>Desulfosporosinus</i>	<i>acidiphilus</i>	SJ4	NC_018068	64	4367	5.80	44
<i>Desulfosporosinus</i>	<i>meridiei</i>	DSM13257	NC_018515	61	4291	4.41	50
<i>Desulfosporosinus</i>	<i>orientis</i>	DSM765	NC_016584	64	5177	5.72	46
<i>Desulfotalea</i>	<i>psychrophila</i>	LSv54	NC_006138	51	3065	3.63	37
<i>Desulfotignum</i>	<i>phosphitoxidans</i>	DSM13687	NZ_APJX00000000	57	4589	9.92	25
<i>Desulfotomaculum</i>	<i>acetoxidans</i>	DSM771	NC_013216	56	3989	5.91	48
<i>Desulfovibrio</i>	<i>desulfuricans</i>	ATCC27774	NC_011883	55	2299	4.80	28
<i>Desulfovibrio</i>	<i>desulfuricans</i>	ND132	NC_016803	54	3399	2.88	42
<i>Desulfovibrio</i>	<i>vulgaris</i>	DP4	NC_008751	56	2885	2.64	39
<i>Desulfovibrio</i>	<i>vulgaris</i>	Hildenborough	NC_002937	56	3322	2.68	37
<i>Desulfovibrio</i>	<i>vulgaris</i>	RCH1	NC_017310	53	3013	2.59	38
<i>Desulfurococcus</i>	<i>kamchatkensis</i>	1221n	NC_011766	64	1406	1.53	104
<i>Thermococcus</i>	<i>litoralis</i>	DSM5473	NC_022084	64	2452	0.67	91
<i>Thermodesulfobacterium</i>	<i>geofontis</i>	OPB45	NC_015682	56	1539	4.08	80
<i>Thermodesulfobium</i>	<i>narugense</i>	DSM14796	NC_015499	53	1753	8.93	51
<i>Thermodesulfovibrio</i>	<i>yellowstonii</i>	DSM11347	NC_011296	54	1974	6.18	63

**Table 2**  
Literature generation time (GT) and optimal growth temperature for 11 SRM.

Genome	Measured Generation Time (hours)	Measured opt. Temperature (°C)	References
Archaeoglobus_profundus_DSM_5631_uid43493	6.3	88	Zhou et al. (2011)
Archaeoglobus_sulfatcallidus_PM70_1_uid201033	2.0	84	Steinsbu et al. (2010)
Desulfatibacillum_alkenivorans_AK_01_uid58913	28.4	27	Ming So and Young (1999)
Desulfococcus_oleovorans_Hxd3_uid58777	96.0	22	Savage et al. (2010)
Desulfosporosinus_acidiphilus_SJ4_uid156759	14.0	55	Alazard et al. (2010)
Desulfovibrio_desulfuricans_ATCC_27774_uid59213	10.2	30	Herrera et al. (1991)
Desulfovibrio_desulfuricans_ND132_uid63159	5.0	35	Gilmour et al. (2011)
(Crenarch) Desulfurococcus_kamchatkensis_1221n_uid59133	1.5	85	Kublanov et al. (2009)
Sulfurimonas_denitrificans_DSM_1251_uid58185	12.0	33	Takai et al. (2006)
Thermodesulfobacterium_OPB45_uid68283	5.0	83	Hamilton-Brehm et al. (2013)
Thermodesulfobium_narugense_DSM_14796_uid66601	12.0	55	Mori et al. (2003)

3–5500  $\mu\text{M}$  (Pallud and Van Cappellen, 2006; Tarpgaard et al., 2011). These kinetic studies were conducted with pure cultures, sediments or sediment slurries, with different experimental approaches such as progress curve experiments and initial velocity experiments. Each type of kinetic experiment is associated with potential experimental artifacts that need to be taken into consideration (Roychoudhury et al., 1998; Pallud and Van Cappellen, 2006). For example,  $K_s$  values measured in sediment slurries have been shown to be higher than the measurements in intact sediment (Fukui and Takii, 1994; Pallud and Van Cappellen, 2006). In our work, we focus on  $K_s$  values derived from kinetic experiments involving pure marine and freshwater SRM cultures. Particularly those that can also be found in the original set of twenty-five: *Archaeoglobus fulgidus* (Habicht et al., 2005), *Desulfobacter postgatei* (Ingvorsen et al., 1984), *Desulfovibrio desulfuricans* (Okabe et al., 1992; Dalsgaard and Bak, 1994), *Desulfovibrio vulgaris* (Ingvorsen and Jørgensen, 1984; Nethejaenchen and Thauer, 1984), *Thermodesulfobacterium* sp (Sonne-Hansen et al., 1999) and *Thermodesulfovibrio* sp (Sonne-Hansen et al., 1999).

Of the twenty-five SRM listed in Table 1, eleven have been identified in oil reservoirs in the North Sea region. *Archaeoglobus fulgidus*, *A. profundus*, *Thermococcus litoralis* are hyperthermophilic SRMs that were isolated from Thistle offshore oil production platform in East Shetland Basin (Stetter et al., 1993). SRMs of the genus

*Thermodesulfobacterium* and *Desulfotomaculum* are thermophilic SRMs also from oil production platforms in the North Sea (Christensen et al., 2012; Rosnes et al., 1991). Mesophilic SRM from the North Sea region have also been identified belonging to the genus *Desulfobulbus* (Lien et al., 1998), *Desulfotignum* (Ommedal and Torsvik, 2007), *Desulfobacter* (Lien and Beeder, 1997), *Desulfomicrobium* and *Desulfovibrio* (Dahle et al., 2008).

## 2.2. Model description

To simulate the multiphase flow and bio-chemical reactions needed for the model, we chose TMVOC\_REACT (Zheng et al., 2013), a simulator that combines TMVOC (Pruess and Battistelli, 2002) and TOUGHREACT (Xu et al., 2011). TOUGHREACT is a numerical simulation program for chemically reactive nonisothermal flows of multiphase fluids in porous and fractured media. A variety of subsurface thermo-physical-chemical-biological processes are considered under a wide range of hydrological and geochemical conditions. In TMVOC\_REACT, the fluid and heat flow simulator in TOUGHREACT was replaced with TMVOC, a numerical simulator for three-phase nonisothermal flow of multicomponent hydrocarbon mixtures in variably saturated heterogeneous media. In the TMVOC formulation, the multiphase system is assumed to be composed of water, noncondensable gases (NCGs), and non-aqueous phase

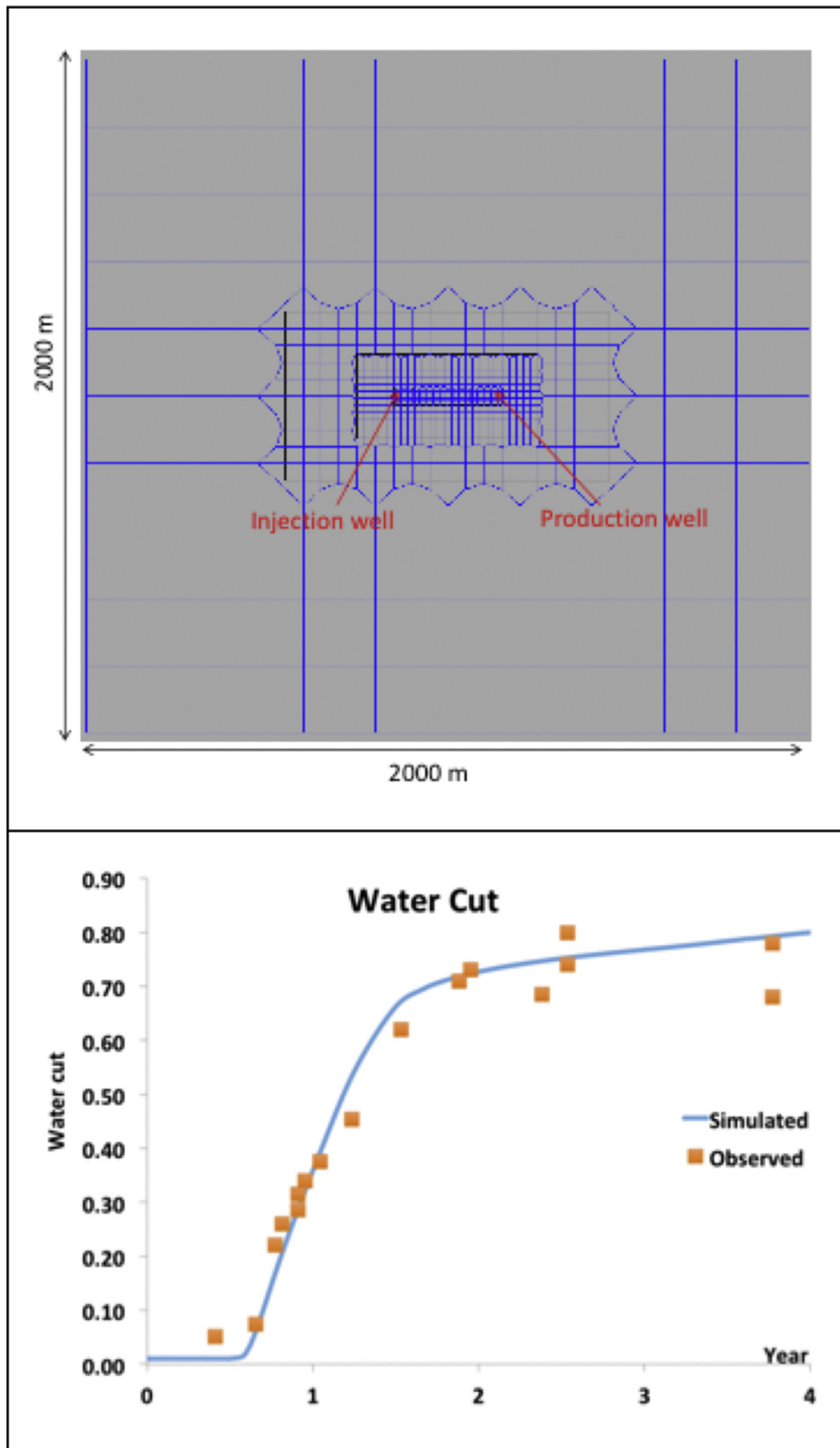


Fig. 1. (a, top) Mesh used in the model and the position of wells. (b, bottom) Simulated water cut trend and water cut data from an undisclosed site in the North Sea region.

liquids (NAPL) including water-soluble volatile organic chemicals (VOCs). The number and nature of NCGs and VOCs can be specified by the user. The fluid components may partition (volatilize and/or dissolve among gaseous, aqueous, and NAPL phases). Any combination of the three phases may be present, and phases may appear and disappear in the course of a simulation. The routine GASEOS (Moridis et al., 2008) was incorporated into TMVOC\_REACT for computation of multi-component gas mixture properties, including parameters and formulations for the phase partitioning of toluene and H<sub>2</sub>S in addition to CO<sub>2</sub>. The GASEOS routine incorporates several standard cubic equations of state such as Redlich-Kwong (RK), Peng-Robinson (PR), and Soave-Redlich-Kwong (SRK) (e.g., Orbey and Sandler, 1998). The partition of H<sub>2</sub>S in gas and aqueous phase is based on Duan et al. (2007) in which solubility of H<sub>2</sub>S is the function of salinity, pressure and temperature. The partition of H<sub>2</sub>S between oil and aqueous phase is a function of temperature and pressure.

The model simulates a hypothetical reservoir (with characteristics based on an undisclosed North Sea fractured sandstone reservoir) with one injection well and one production well. A modeling domain of 2000 m × 2000 m in horizontal direction was discretized into 642 elements (Fig. 1a). The vertical direction extends 90 m without discretization, corresponding to a reservoir of 90 m thick. The injection and production wells are 250 m apart and connected via a fracture zone. The area around the wells is made up of finely discretized cells as shown in Fig. 1a. A constant injection and production rate of 11 kg/s is assumed in the model in order to capture

components in the oil phase, with *n*-Decane being the dominant one. The initial pressure is 191 bars and temperature is 69.4 °C.

Concentrations of aqueous species in the formation water (FW) and the injection water (IW) follow those in Hubbard et al. (2014). The initial concentrations of aqueous species matched that of the formation water (FW) found in sample #158 from Warren et al. (1994). This sample was taken from the Brent sandstone reservoir in the Oseberg Field of the northern province of the North Sea. The carbon source in the simulation was represented simply as toluene, at a concentration of 1% mass fraction in the formation oil (typical for light crudes from the North Sea, data based on Statoil, 2015). For the injection water (IW), we assumed an operating scenario of produced water reinjection (e.g. Haghshenas et al., 2012), where the injection water was a mixture of 75% seawater (SW) and 25% FW, i.e. IW = 0.75 SW + 0.25 FW. An additional source of nitrogen was introduced as 1.0 mmol/kg H<sub>2</sub>O (18 mg L<sup>-1</sup>) ammonium bisulfite (NH<sub>4</sub>HSO<sub>3</sub>), which is a common chemical used to scavenge oxygen from injection waters in order to minimize oxygen corrosion (Kelland, 2009). We have assumed that all the bisulfate is transformed to sulfate by reaction with oxygen. For simplicity, the injection water was kept constant in each simulation i.e. not adjusted to reflect temporal changes in the produced water, which are characteristic of actual operating oil fields. Detailed aqueous species concentrations in FW, SW and IW can be found in Table 3.

The kinetics of the microbial population are mathematically described by the following general Monod equation:

$$r = \frac{\mu_{MAX} f(T) [\text{Biomass}] ([\text{eDonor}])}{[\text{eDonor}] + K_S^{\text{eDonor}}} \frac{[\text{eAcceptor}]}{[\text{eAcceptor}] + K_S^{\text{eAcceptor}}} \frac{K_S^{\text{Inhibitor}}}{[\text{Inhibitor}] + K_S^{\text{Inhibitor}}} \quad (3)$$

the watercut trend from an undisclosed site in the North Sea region (Fig. 1b). The fracture zone in the reservoir is coarsely represented as a single fracture, and has a porosity of 0.03 and a permeability of  $2 \times 10^{-10}$  m<sup>2</sup>, whereas the rocks surrounding the fracture zone have a porosity of 0.13 and a permeability ranging from  $7 \times 10^{-14}$  m<sup>2</sup> to  $1 \times 10^{-11}$  m<sup>2</sup>. The relative permeability for the fracture zone and surrounding rocks takes Corey's curve (Corey, 1954):

$$K_{rl} = \hat{s}^4 \quad K_{ro} = (1 - \hat{s})^2 (1 - \hat{s}^2) \quad (2)$$

where  $K_{rl}$  and  $K_{ro}$  are relative permeability for aqueous and NAPL phase, respectively, and  $\hat{s} = (s_l - s_{lr}) / (1 - s_{lr} - s_{lo})$  where  $s_{lr}$  and  $s_{lo}$  are residual aqueous and NAPL saturation.

The NAPL phase is approximating a light oil that has a density around 670 kg/m<sup>3</sup>. H<sub>2</sub>S, toluene, *n*-Hexane and *n*-Decane are four

where  $r$  (mol/kg H<sub>2</sub>O/sec) is the reaction rate,  $f(T)$  is a temperature function that modulates the growth rate of the SRM population (see below), [Biomass] (mol/kg H<sub>2</sub>O) is the concentration of the microbial biomass catalyzing the reaction,  $\mu_{MAX}$  (sec<sup>-1</sup>) is the maximum specific growth rate,  $K_S$  (mol/kg H<sub>2</sub>O) is the half saturation (affinity constant) of the electron donor/acceptor/inhibitor. Following the concepts as described by Rittman and MaCarty (2001), microbially mediated reactions are divided into two components: catabolic and anabolic. For each mole of electron donor/substrate utilized, a fraction,  $f_s$ , is conserved by the microbial biomass for cell synthesis (anabolic) while the remaining fraction,  $f_e$ , is used for energy production (catabolic). Values of  $f_s$  and  $f_e$  are determined by the types of electron donors and acceptors involved in the reaction (Rittman and MaCarty, 2001). For reduction of sulfate coupled to oxidation of toluene,  $f_e$  and  $f_s$  values are 0.93 and 0.07 respectively, resulting in

**Table 3**

Aqueous species concentrations in Formation Water (FW) and Injection Water (IW). Chemical concentrations in FW and IW used as initial and amendment conditions respectively in TMVOC\_REACT simulation.

Primary Species	Formation Water (mmol/kg H <sub>2</sub> O)	Injection Water (mmol/kg H <sub>2</sub> O)
pH	7.00	7.00
Na <sup>+</sup>	690.00	516.75
K <sup>+</sup>	7.40	9.35
Ca <sup>2+</sup>	21.00	12.75
Mg <sup>2+</sup>	5.10	40.28
SO <sub>4</sub> <sup>2-</sup>	0.04	21.00
Cl <sup>-</sup>	660.00	566.25
CO <sub>2(aq)</sub>	8.66	8.66
H <sub>2</sub> S <sub>(aq)</sub>	0.00	0.00
NH <sub>4</sub> <sup>+</sup>	1.00	1.00
Br <sup>-</sup>	1.48	1.12

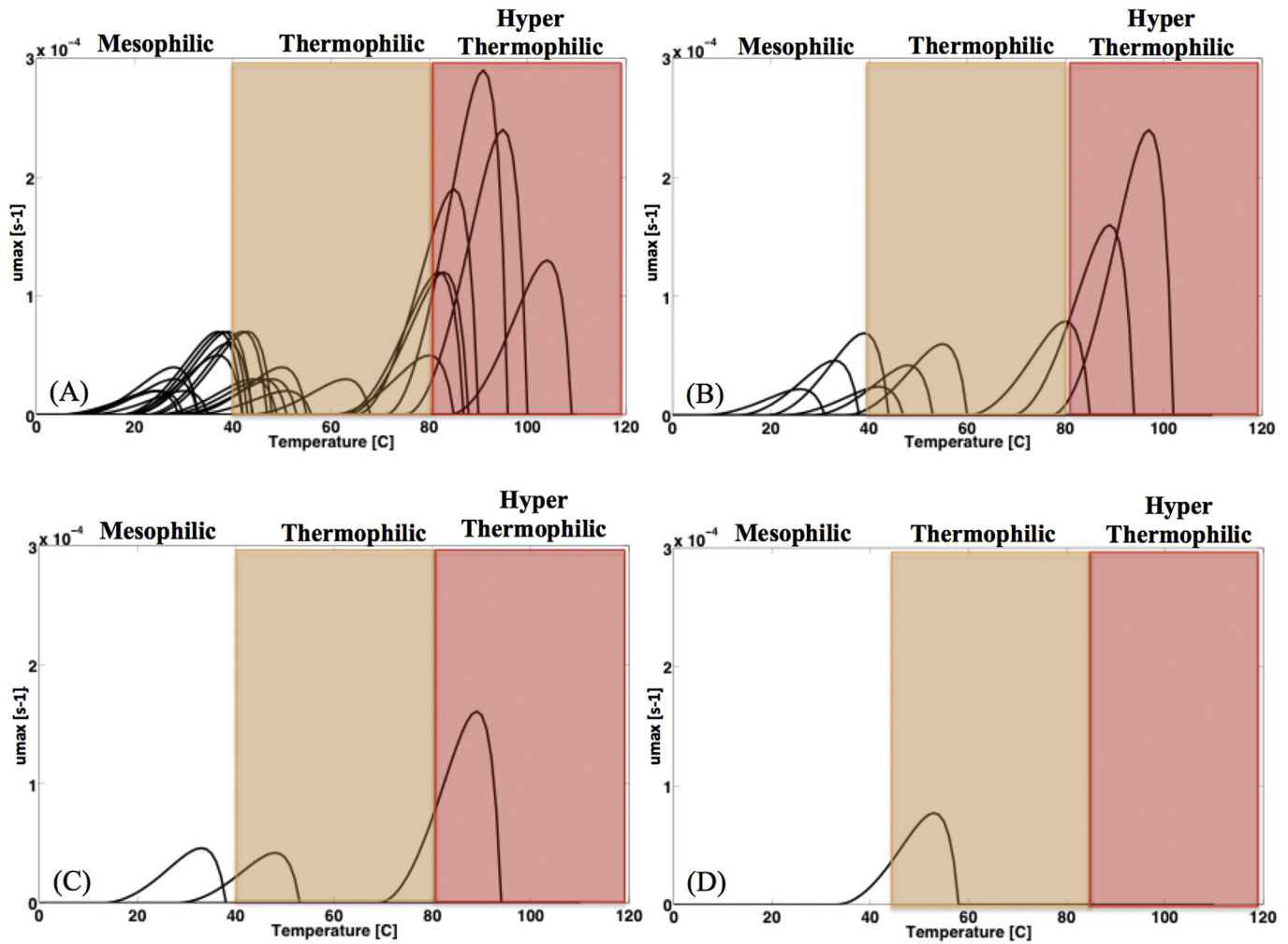
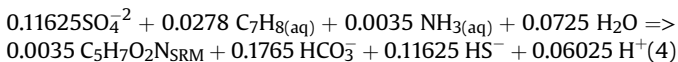


Fig. 2. Maximum growth rates,  $\mu_{MAX}$ , a function of temperature for increasing degrees of sulfate reducer microorganism (SRM) complexity. (A) All 25 SRM represented. (B) Nine SRM guilds, three guilds in each thermal range: mean and  $\pm 1$  standard deviation. (C) Three SRM guilds, one guild in each thermal range. Mean values of all SRM data within the same temperature range. (D) Single SRM guild, mean values of all 25 SRM data.

the following stoichiometric equation:



A stoichiometric formula of  $\text{C}_5\text{H}_7\text{O}_2\text{N}$  is used to represent cell biomass of the SRM in this work. For the choice of this and other stoichiometric formulae, the reader is referred to Rittman and McCarty (2001, Chapter 2, Table 2.4). SRM catalyze the reduction of sulfate to sulfide via the action of intracellular enzymes. Due to the temperature sensitivity of the enzymes, SRM activities are impacted by the reservoir thermal regime. Following the approach of a recent modeling study (Farhadinia, 2008), SRM have been classified according to their temperature optima into three groups: mesophiles (20–40 °C), thermophiles (40–80 °C) and hyperthermophiles (80–113 °C). For each group, temperature effects on growth are modeled according to a previously published function

(Ratkowsky et al., 1983; Rosso et al., 1995). In recognition of the importance of temperature in controlling activities of SRM in the oil reservoir, we have incorporated a temperature function into TMVOC-REACT that will modulate the growth rate of the SRM population. The mathematical formulation of this temperature function follows the Rosso et al. (1995) model. The temperature function behaves in a similar manner as the Ratkowsky curves, and is described by the three parameters: upper limit temperature ( $T_{MAX}$ ), optimal temperature ( $T_{OPT}$ , derived from genomic data) and lower limit temperature ( $T_{MIN}$ ):

$$f(T) = \begin{cases} T < T_{MIN}, 0.0 \\ T_{MIN} < T < T_{MAX}, \eta(T) \\ T > T_{MAX}, 0.0 \end{cases}$$

$$\eta(T) = \frac{(T - T_{MAX})(T - T_{MIN})^2}{(T_{OPT} - T_{MIN})[(T_{OPT} - T_{MIN})(T - T_{OPT})(T_{OPT} - T_{MAX})(T_{OPT} + T_{MIN} - 2T)]} \quad (5)$$

Another important parameter in the Monod equation is the maximum growth rate,  $\mu_{MAX}$ , (see Equation (3)). The mathematical formulation employed to derive  $\mu_{MAX}$  from the minimum generation (doubling) time,  $t$ , as derived from genomic data is as follows:

$$\mu_{Max} = \frac{\ln 2}{t} \quad (6)$$

### 2.3. Model simulations

To explore the degree of complexity necessary to represent the kinetics of SRM community in an oil field, we conducted four sulfate reducing simulation scenarios. In each simulation scenario, the SRM community is made up of different number of members. Below we describe each scenario.

**Scenario A.** Full complexity of the SRM community is represented. All twenty-five SRM are represented (Fig. 2A).

**Scenario B.** The complexity of the SRM community is reduced in comparison to Scenario A. There are a total of nine SRMs. Three SRM within each of the temperature regimes (i.e. mesophilic, thermophilic and hyperthermophilic). One of the SRM is characterized by mean values of  $\mu_{MAX}$ , optimal growth temperature and  $K_S$  derived from the SRM within the corresponding temperature regime in Scenario A. The remaining two SRM are characterized by values of  $\mu_{MAX}$ , optimal growth temperature and  $K_S$  that are  $\pm 1$  standard deviation of the mean (Fig. 2B).

**Scenario C.** There are a total of three SRM. One SRM within each of the temperature regimes. The SRM is characterized by mean values of  $\mu_{MAX}$ , optimal growth temperature and  $K_S$  derived from the SRM within the corresponding temperature regime in Scenario A (Fig. 2C).

**Scenario D.** The kinetics of the SRM community are represented by a single SRM, with a single  $\mu_{MAX}$ , optimal growth temperature and  $K_S$  that are the mean of  $\mu_{MAX}$ , optimal growth temperature and  $K_S$  of all 25 SRM investigated in this work. This resulting SRM guild operates optimally in the thermophilic region (Fig. 2D). This scenario represents typical model representation of SRM in other simple modeling studies.

## 3. Results and discussion

### 3.1. Deriving model parameters from microbial datasets

#### 3.1.1. Comparison between predicted traits and observed traits

We compare minimum generation time and optimal growth temperature derived from genomic data against literature (observed) values for eleven known SRM (Fig. 3). Of the eleven SRM with literature values, five are from the mesophilic regime (*Desulfatibacillum alkenivorans*, *Desulfococcus oleovorans*, *Desulfovibrio desulfuricans*, *Sulfurimonas denitrificans*), two are from the thermophilic region (*Desulfosporosinus acidiphilus*, *Thermodesulfobium narugense*), while the remaining four are from the hyperthermophilic region (*Thermodesulfobacterium* sp., *Desulfurococcus kamchatkensis*, *Archaeoglobus sulfaticallidus*, *Archaeoglobus profundus*). Optimal growth temperature calculated from the frequency of amino acids IVYWREL in the proteome of the SRM (Zeldovich et al., 2007) seems to match literature values with relatively high degree of fidelity (R squared value of 0.86, Fig. 3A). In comparison, minimum generation time, as derived from codon usage bias index (Vieira-Silva and Rocha, 2010) does not match the literature values

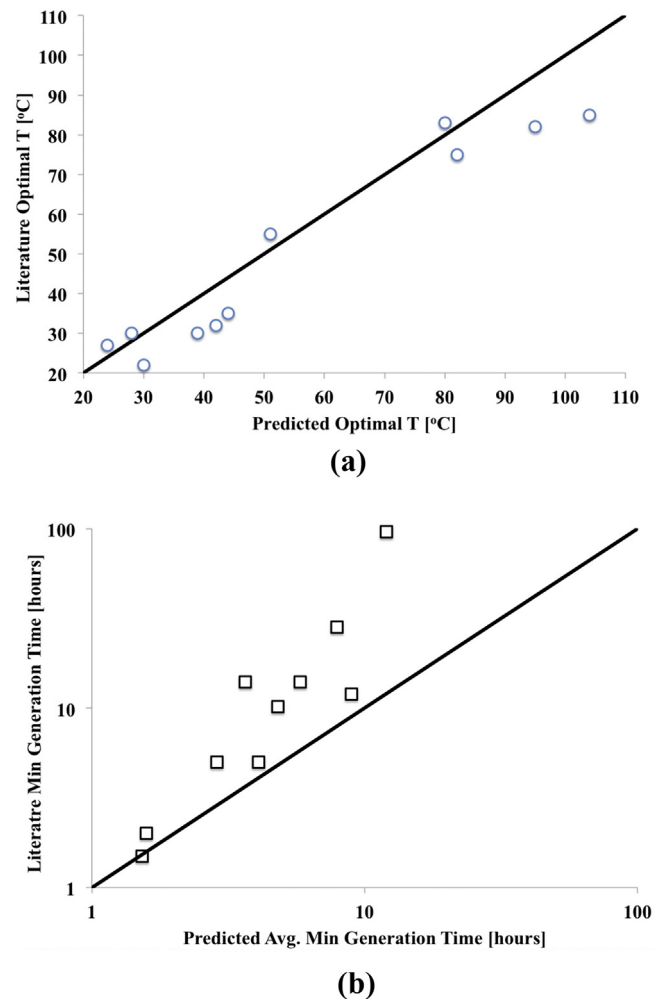


**Fig. 3.** (A) Comparison between literature optimal growth temperature and predicted optimal growth temperature (from genomic data) for 11 SRM. The diagonal black line corresponds to the identity. (B) Comparison between literature minimum generation time and predicted minimum generation time (from genomic data) for 11 SRM. The diagonal black line corresponds to the identity.

with such high degree of fidelity (R squared value of 0.44). The model tends to under-predict minimum generation time, particularly at higher values of minimum generation time (Fig. 3B). In the original study by Vieira-Silva and Rocha (2010), the authors demonstrated codon usage bias to be a better predictor of minimum generation time than other genomic signatures such as number of rRNA operons in the genome. In the Vieira-Silva and Rocha (2010) study, the author predicted the minimum generation time of 214 prokaryotes. The R squared value between the predicted minimum generation time and literature values is 0.58. Their study also showed that the observed generation time for thermophiles used in their study, is higher than values derived from the genomic signatures.

#### 3.1.2. Relationships between traits

We plot minimum generation time,  $K_S$  and optimal growth temperature to explore the relationship between these three traits (Fig. 4).

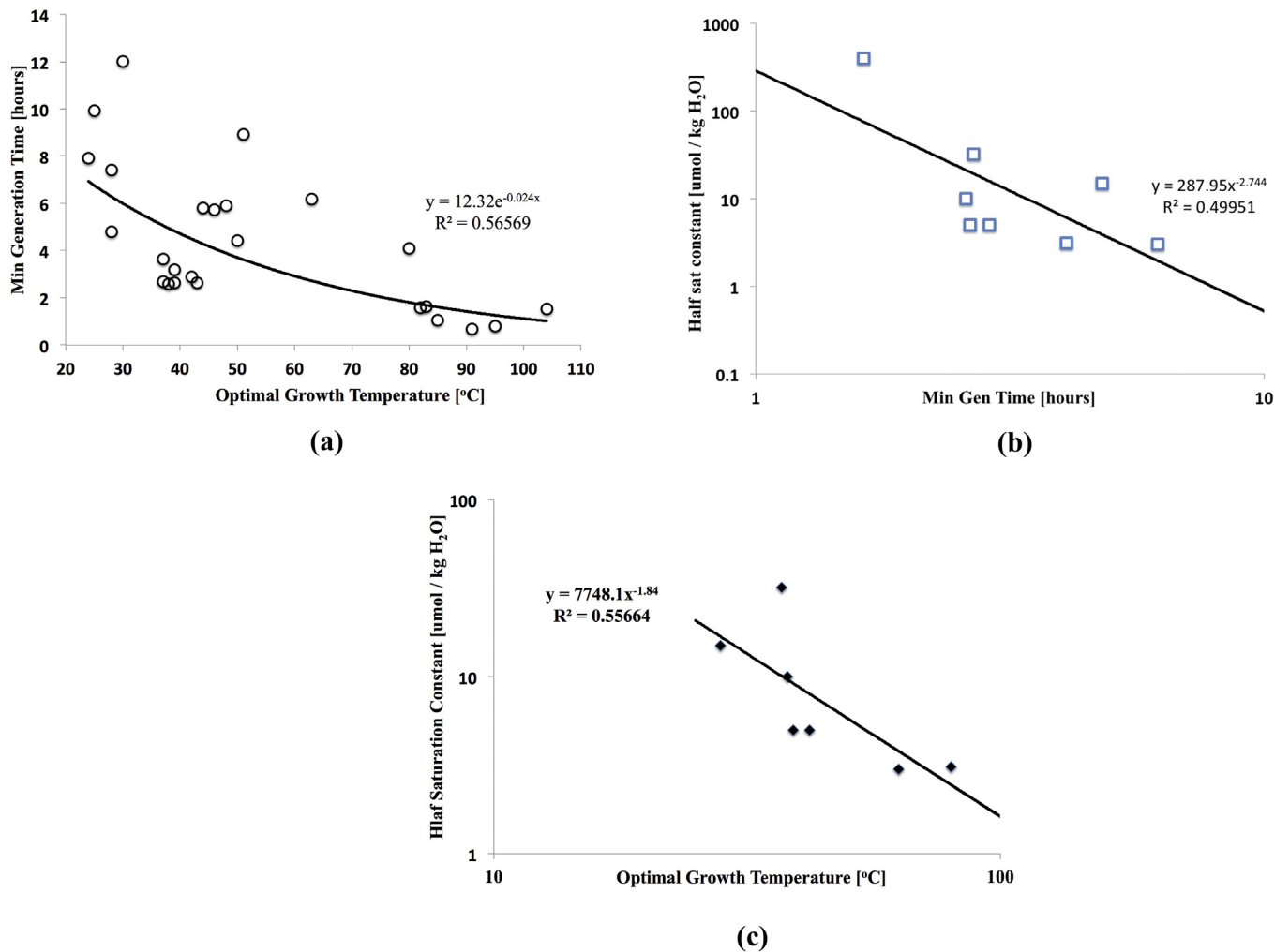


Fig. 4. (A) Relationship between min generation time and optimal growth temperature. (B) Relationship between half saturation constant and minimum generation time. (C) Relationship between optimal growth temperature and half saturation constant.

3.1.2.1. Minimum generation time and optimal growth temperature.

While results suggest negative relationship between minimum generation time and optimal growth temperature (R squared value of 0.57, Fig. 4A), the correlation is not a strong one. Our current finding with SRM literature values is similar to the observations made by Vieira-Silva and Rocha (2010). From their data they found no significant difference of minimal generation times between thermophiles, mesophiles and psychrophiles.

3.1.2.2.  $K_s$  and minimum generation time.

While our data suggest a weak relationship between  $K_s$  and minimum generation time for SRM (R squared value of 0.5, Fig. 4B), such relationship has been shown to exist in other microorganisms. The  $K_s$  and  $\mu_{MAX}$  (derived from minimum generation time using Equation (6)) trade off is also known as the r-K strategy dichotomy (MacArthur and Wilson, 1967; Sommer, 1981). Populations that are accustomed to disturbances and/or feast-and-famine lifestyles due to intermittent nutrient influxes are r-strategists. The r-strategists are opportunistic and are characterized by high growth rates. On the other hand, the K-strategists are populations that thrive in environments with more stable nutrient concentrations. These K-strategists are also known as equilibrium populations and have high competitive ability (e.g. high substrate affinity) (Andrews

Temperature evolution (Injection: 30°C, Formation: 70°C).

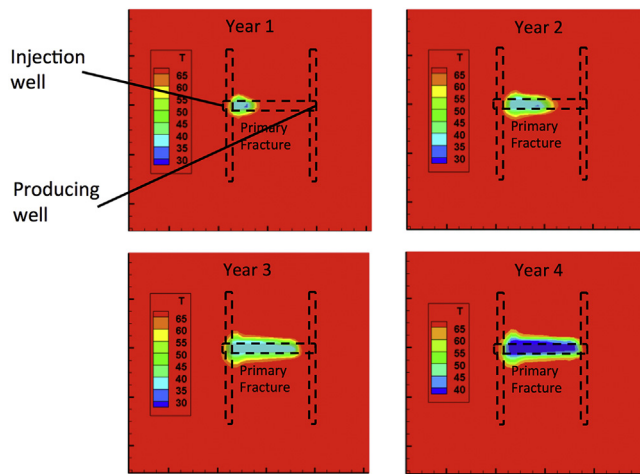


Fig. 5. Spatial distribution of reservoir temperature (unit = °C) from the beginning of the water injection to Year 4. The temperature of the oil reservoir (formation) is 70 °C while that of the injection water is 30 °C.

and Harris, 1986). When determining the vertical distribution of two bacterial populations in a stratified lake, Weinbauer and Hofle (1998) also characterized the life strategies of these two populations, namely *Comamonas acidovorans* PX54 and *Aeromonas hydrophila* PU7718. Their study revealed that *A. hydrophila* PU7718 is an r-strategist with high growth rate, while *C. acidovorans* PX54 with lower growth rate but high substrate affinity and resistance to grazing is a K-strategist. Evidence supporting this trade-off relationship can also be found in phytoplankton community studies (Litchman and Klausmeier, 2008). Green algae with high maximum growth rate dominate high nutrient lakes, while phytoplanktons with low maximum growth rates but high substrate affinity (low  $K_s$ ) tend to dominate water bodies with low nutrient concentrations (Reynolds,

2006).

3.1.2.3.  $K_s$  and optimal growth temperature. Our result suggests a negative relationship between  $K_s$  and optimal growth temperature (R squared value of 0.56, Fig. 4C).  $K_s$ , as a property of the quaternary enzyme structure, is inherently influenced by temperature (Somero, 2004; Koch et al., 2007; German et al., 2012), although the response can be irregular (Stone et al., 2012). Adjustment of the amino acid composition modifies the protein structure resulting in enzyme acclimation to an optimal local temperature. The result of this modification is to render the protein structure more rigid at higher temperatures (Johns and Somero, 2004) with a lower effective  $K_s$  (and higher affinity), relative to mesophilic conditions. This relationship is used in the

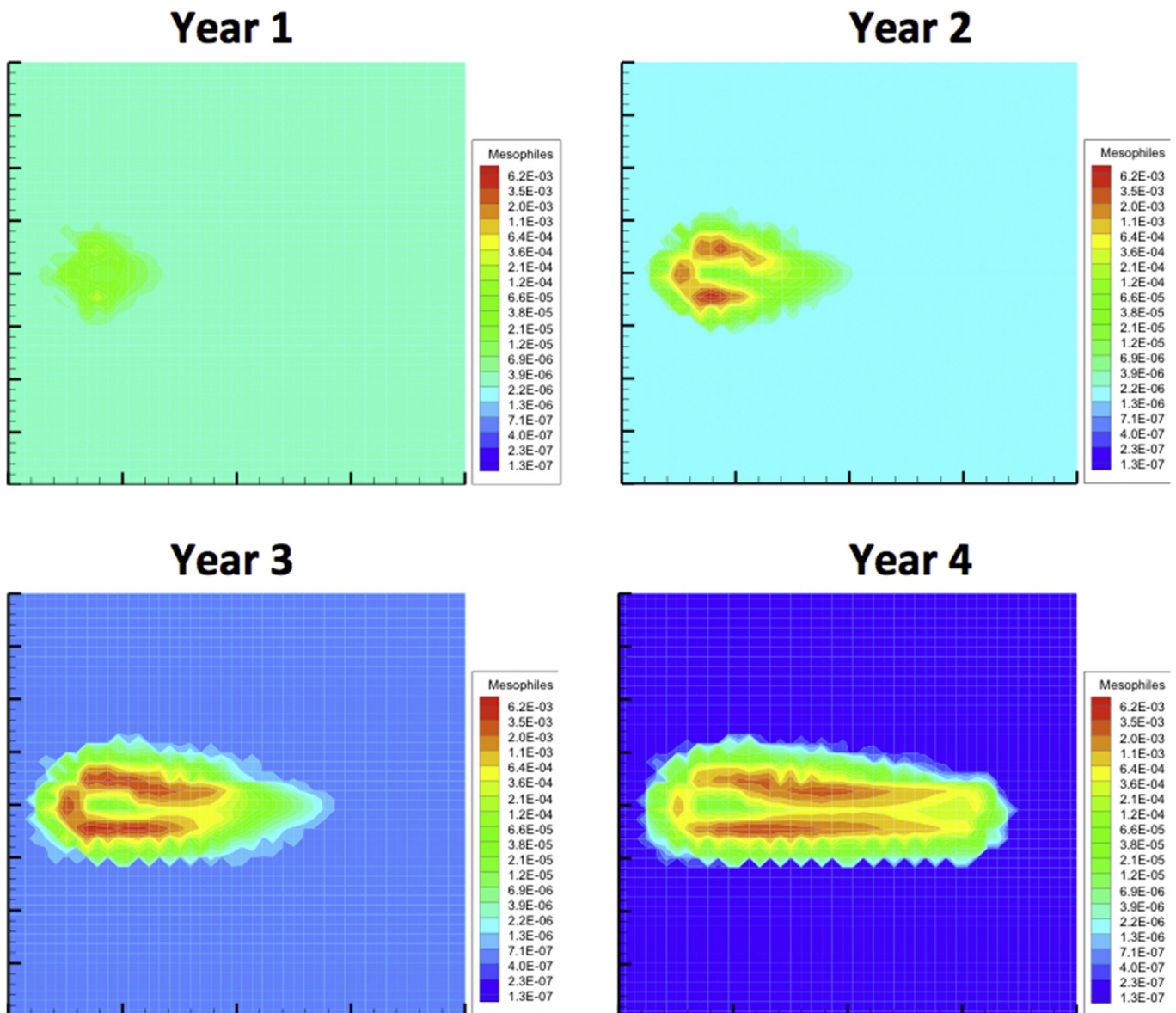


Fig. 6. Spatial distribution of mesophiles (unit = mol kgw<sup>-1</sup>) from the beginning of the water injection to Year 4.

derivation of  $K_s$  values that were unavailable for some of the twenty-five SRM in the simulations. In comparison to the relationship between  $K_s$  and minimum generation time, this relationship has higher R squared value. Further, optimal growth temperature derived from genomic data match literature values with relatively high degree of fidelity than minimum generation time.

### 3.2. Simulation results

#### 3.2.1. Temperature impact on the emergence of the SRM community composition

The integrated model simulated the injection of a relatively cold seawater and produced water mix into the injection well of the reservoir. The formation temperature of 70 °C in the model

mimics the formation temperature found on site. The model captured the four-year watercut trend (data) from an undisclosed site in the North Sea region (Fig. 1b). Cold water (30 °C) injected lowered the temperature of the region surrounding the injection well rapidly to 36 °C within the first year. The injected water preferentially flowed along the primary fracture connecting the injection well and the producing well. Breakthrough occurred at around the first half year. As a result, a thermal gradient began to develop along the primary fracture. The gradient varied year to year, from 70 °C (producing well) to 37 °C (injection well) at Year 1, to 45 °C (producing well) to 37 °C (injection well) at Year 4 (Fig. 5). These hydrologic and thermal conditions are maintained for all the four field scale simulation scenarios investigating SRM community complexity (as described in section 2.3). The simulated thermal gradient follows

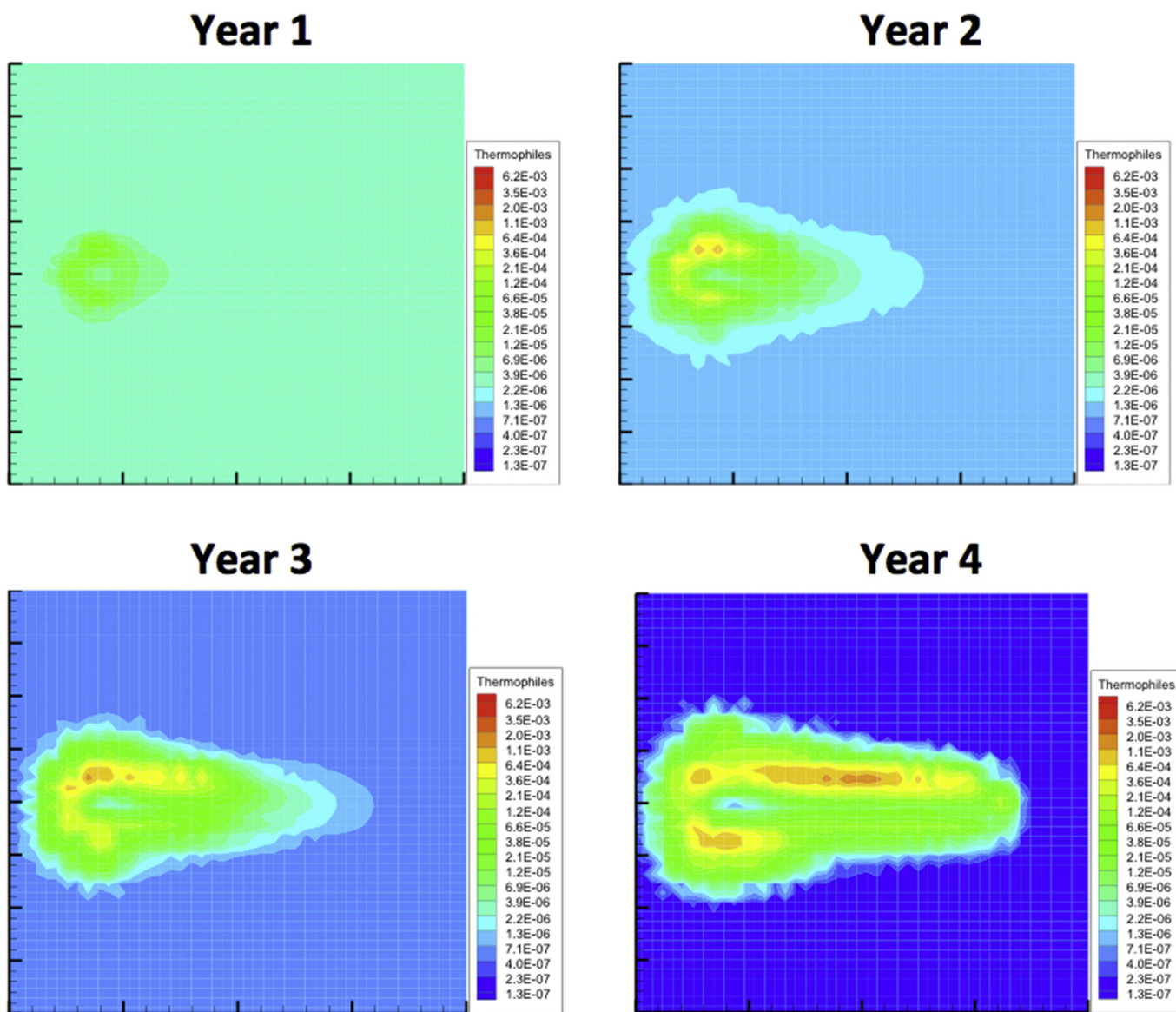


Fig. 7. Spatial distribution of thermophiles (unit = mol kgw<sup>-1</sup>) from the beginning of the water injection to Year 4.

the observed thermal gradient on site (29–66 °C), which straddles mesophile to hyperthermophile range.

Here we discuss the shift in SRM community structure for the field scale simulation involving the twenty-five ecotypes of SRM (**Scenario A**). The SRM community shifted in response to the change in temperature. Initial conditions prescribed the SRM abundance equally throughout the reservoir domain, and as the temperature dropped at the injection well an SRM community dominated by the mesophiles emerged as early Year 2 (**Figs. 6–8**). Deeper into the rock matrix in the oil reservoir, temperature only begun to fall after Year 2.5. At Year 4, the temperature at the producing well was at 45 °C. While this temperature is conducive for the thermophiles, they did not overtake the hyperthermophiles as the dominant until ~6 months later (**Fig. S1**). (Note: simulation for **Scenario A** was extended by a year to show the shift in SRM community as the temperature at the producing well continues to fall) At Year 5,

temperature at the producing well is ~37 °C, the thermophiles have taken over the hyperthermophiles as the dominant population. However, with time, as the temperature remain conducive for the mesophiles, we can expect the mesophiles to dominate.

### 3.2.2. Comparison between the different simulation scenarios

We compare the effluent sulfate and sulfide concentrations between the four field scale simulations (**Fig. 9**), using scenario A (25 SRM) as the baseline for comparison. Effluent sulfate and sulfide from **Scenario A** (25 SRM) and **B** (9 SRM) closely matched each other, while effluent sulfate and sulfide from **scenario C** (3 SRM) and **D** (1 SRM) closely matched each other. Effluent sulfate broke through at the producing well and rose rapidly to 21 mmol kg<sup>-1</sup> (the concentration in the injection water) in all four scenarios by Year 1. From then on, the effluent sulfate concentrations of **scenarios C and D** diverged from those of **scenarios A and B**. From Year 1.5 to Year 4, effluent sulfate concentrations of

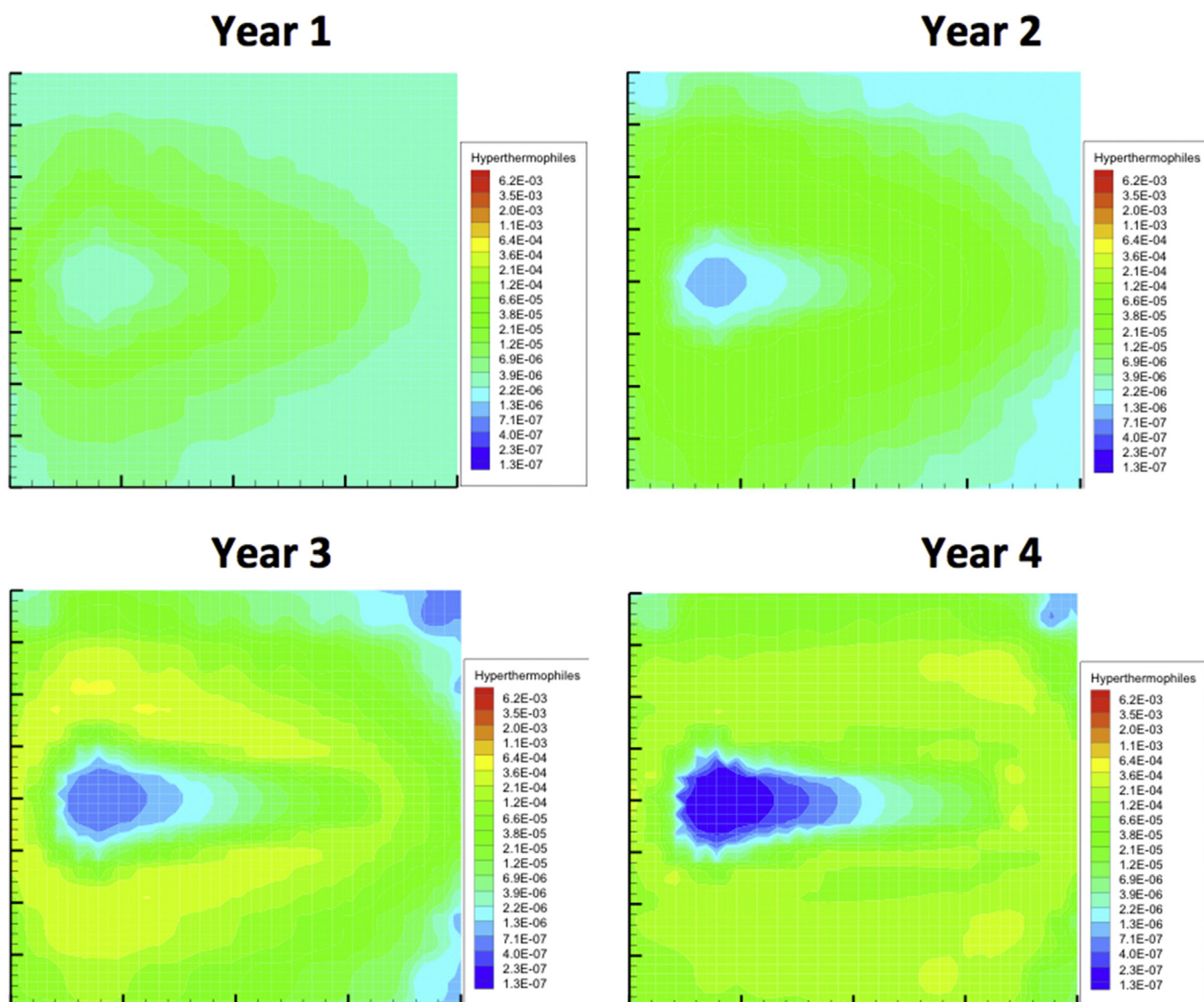


**Fig. 8.** Spatial distribution of hyperthermophiles (unit = mol kg<sup>-1</sup>) from the beginning of the water injection to Year 4.

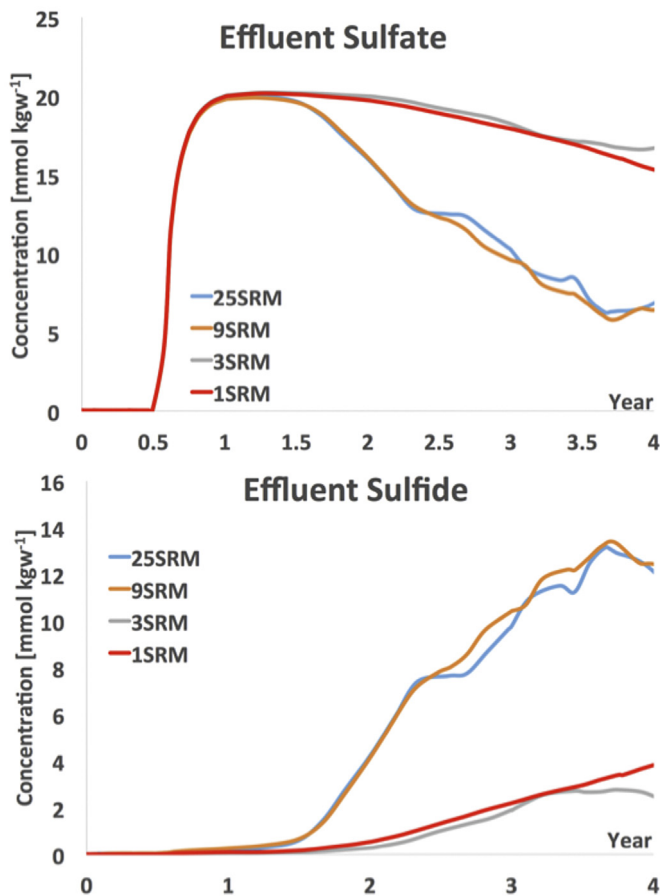


Fig. 9. (TOP) Comparison of effluent sulfate from the four different simulation scenarios. (BOTTOM) Comparison of effluent sulfide from the four different simulation scenarios.

scenario C and D decreased slowly from 21 mmol kgw<sup>-1</sup> to 15 mmol kgw<sup>-1</sup>, while that of scenario A and B decreased more rapidly from 21 mmol kgw<sup>-1</sup> to 6 mmol kgw<sup>-1</sup>. Interestingly, the results demonstrate that the dynamics of the 25 SRM (scenario A) can be replicated by the 9 SRM (scenario B). In contrast, representing the community with only 1 SRM or 3 SRM (one in each temperature regime) cannot sufficiently capture the dynamics of the full SRM community. In fact, the 1 SRM and 3 SRM representations underestimated the bulk sulfate reduction rate of the system compared with the 9 and 25 SRM scenarios (Fig. 9). We further evaluate model performance of scenarios B–D by evaluating root-mean-square errors (RMSEs),  $\sigma$ :

$$\sigma = \sqrt{\frac{\sum_{i=1}^N (C_o^i - C_s^i)^2}{N}} \quad (7)$$

where  $C_o^i$  is the simulated effluent sulfate concentration from scenario A,  $C_s^i$  is the simulated effluent sulfate concentration from the remaining scenarios and  $N$  is the total number of data points. The RMSEs for scenarios B, C and D are 0.33, 4.86 and 4.41 (mmol kgw<sup>-1</sup>) respectively. The RMSE values for scenarios B, C and D are calculated by assuming scenario A as the case which high degree of SRM population complexity is incorporated, which other scenarios

are benchmarked against.

Next we compare the shifts in relative abundance in the SRM community between scenarios A, B and C. At the injection well, temperature rapidly declined from 70 °C to 35 °C within the first half year. The SRM community responded to the temperature shift, and the mesophiles dominated sulfate reduction from 0.5 years on. This trend held for all three scenarios (Fig. 10). Temperature at the producing well remained at 70 °C for the first two years, then slowly declined to 45 °C by the fourth year (Fig. 11). For scenarios A and B, the hyperthermophiles became the dominant population at the producing well within the first year and continued their dominance in terms of cell numbers through to the fourth year. This guild of hyperthermophiles thrive at optimal temperatures in the low 80°Cs, with minimum temperature (for growth) below 70 °C (Fig. 2). While the temperature at the producing well may not be at their optimal temperature, these hyperthermophiles remain competitive since their  $\mu_{MAX}$  values at 70 °C are similar in magnitude to the  $\mu_{MAX}$  values of the thermophiles (scenarios A and B, Fig. 2). For scenario A (25 SRMs), the hyperthermophiles belong to the genus *Archaeoglobus* (*fulgidus* and *sulfatcallidus*) and *Thermodesulfobacterium*. On the other hand, the SRM community in scenario C behaves differently than those from scenarios A and B. The relative abundance of the three guilds (mesophiles, thermophiles, hyperthermophiles) remained constant till Year 3.5, while the temperature of the reservoir was in the range ~50–70 °C. Within this temperature range, none of the 3 SRM guilds derived from the original 25 are capable of growth (see section 2.3 and Fig. 2C). As the temperature drops further (towards 40 °C), the temperature became conducive for the thermophiles, and they increase in relative abundance by Year 4.

Simulation results suggest the possibility of reducing model complexity while maintaining dynamics of the target microbial community. Multi-year reactive transport simulations of oil reservoir dynamics are computational intensive even without the inclusion of microbial kinetics. The incorporation of microbial kinetics adds to the computational burden. Our simulations focus solely on sulfate reduction, which already involve 25 SRM. If other microbially mediated reactions in the oil reservoirs, e.g. biodegradation of oil (Head et al., 2003) and sulfide oxidation, are to be taken into consideration, a far greater number of model parameters would be involved and longer computational run times could be expected. Our simulation results demonstrate a trade off between community complexity and simulation run time. When compared with the 25 SRM simulation, the 1, 3 and 9 SRM simulations took a factor of 0.42, 0.42 and 0.58 times shorter to run respectively. Actual computational for each scenario can be found in Table S1. While representing the SRM community as a single SRM yields the fastest run time, it also yields the highest degree of error. In this work, we systematically reduced microbial community complexity and determined a reduced number of SRMs that was able to capture the kinetics of the full 25 SRM community, with shorter computational runtime.

Here we discuss caveats of the current model. The focus of this study is the exploration of the impacts of representing diversity within SRM community through trait-based modeling coupled to a simplified reactive transport model, and how we can parameterize the kinetic parameters from genomic data (especially in times when data are not available from physiological studies). As such only microbial sulfate reduction are incorporated into this model. In addition to sulfate reducers,

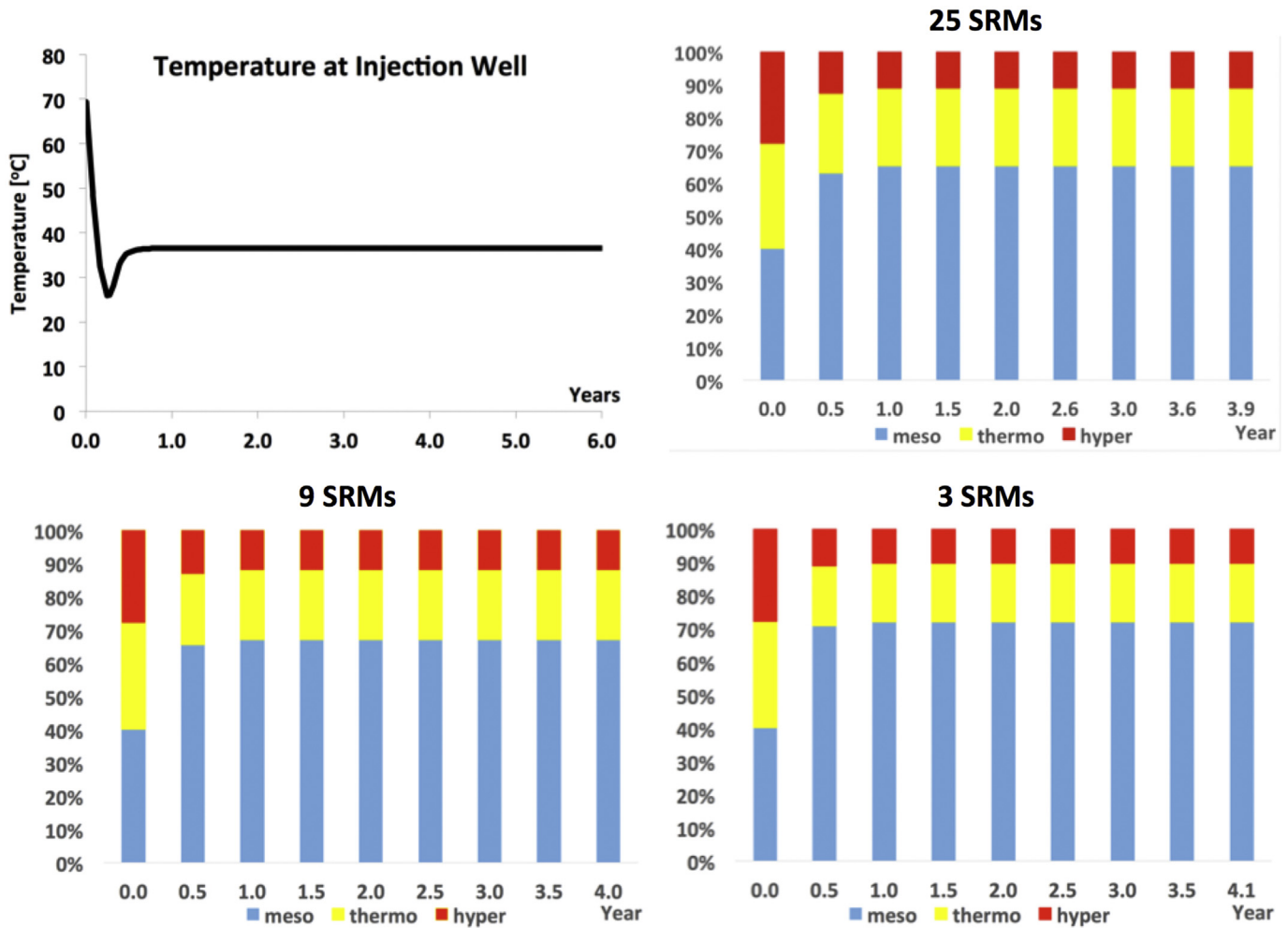


Fig. 10. Comparison of the temporal trends of mesophiles, thermophiles and hyperthermophiles distribution at the injection well between the different scenarios.

other key anaerobic bacteria and archaea have been isolated from oil reservoirs: fermentative heterotrophic bacteria, iron reducing bacteria and methanogenic archaea (Head et al., 2003). Sulfate reducers have been known to interact with other microbial guilds in the deep subsurface. One example is the fermenters (acid producing bacteria). Microbial fermentation produces acetate and other fatty acids, which function as electron donors in sulfate reduction. Further, acid produced by the acid producing bacteria impact the environment by altering pH. Finally, in this work, partitioning of  $H_2S$  between the gas, oil and water phases are dependent on the pressure. Recently, pH has been identified as an important factor controlling the partitioning of  $H_2S$  (Burger et al., 2013) and needs to be considered.

#### 4. Conclusion

In this study, we first showed how genomic information could be used to parameterize the generation time and optimal growth temperature required for modeling microbial souring, and provided a pathway for using microbial data derived from oil reservoir

studies. Of the two parameters, optimal growth temperature (derived from genomics data) matched the literature data with the highest degree of accuracy.

Next, we demonstrated how these derived parameters could be used in a reactive transport simulation of seawater injection into a reservoir. Model with diverse sulfate reducing microbial community represented shifts in community composition as an emergent property that constantly evolves as communities self-organize in response to changing environmental conditions. Finally, we explored the question of necessary model complexity by comparing model results using different numbers of sulfate reducers. Simulation results showed that the kinetics of the 25 SRM could be adequately represented by 9 SRM (with parameter values derived from the mean and standard deviations of the 25 SRM). Importantly, this reduction in complexity from 25 to 9 SRM decreased simulation run time by a factor of ~2. However, further simplification of the community to 3 or 1 SRM could not reproduce the souring dynamics, highlighting the importance of adequately capturing system complexity in modeling.

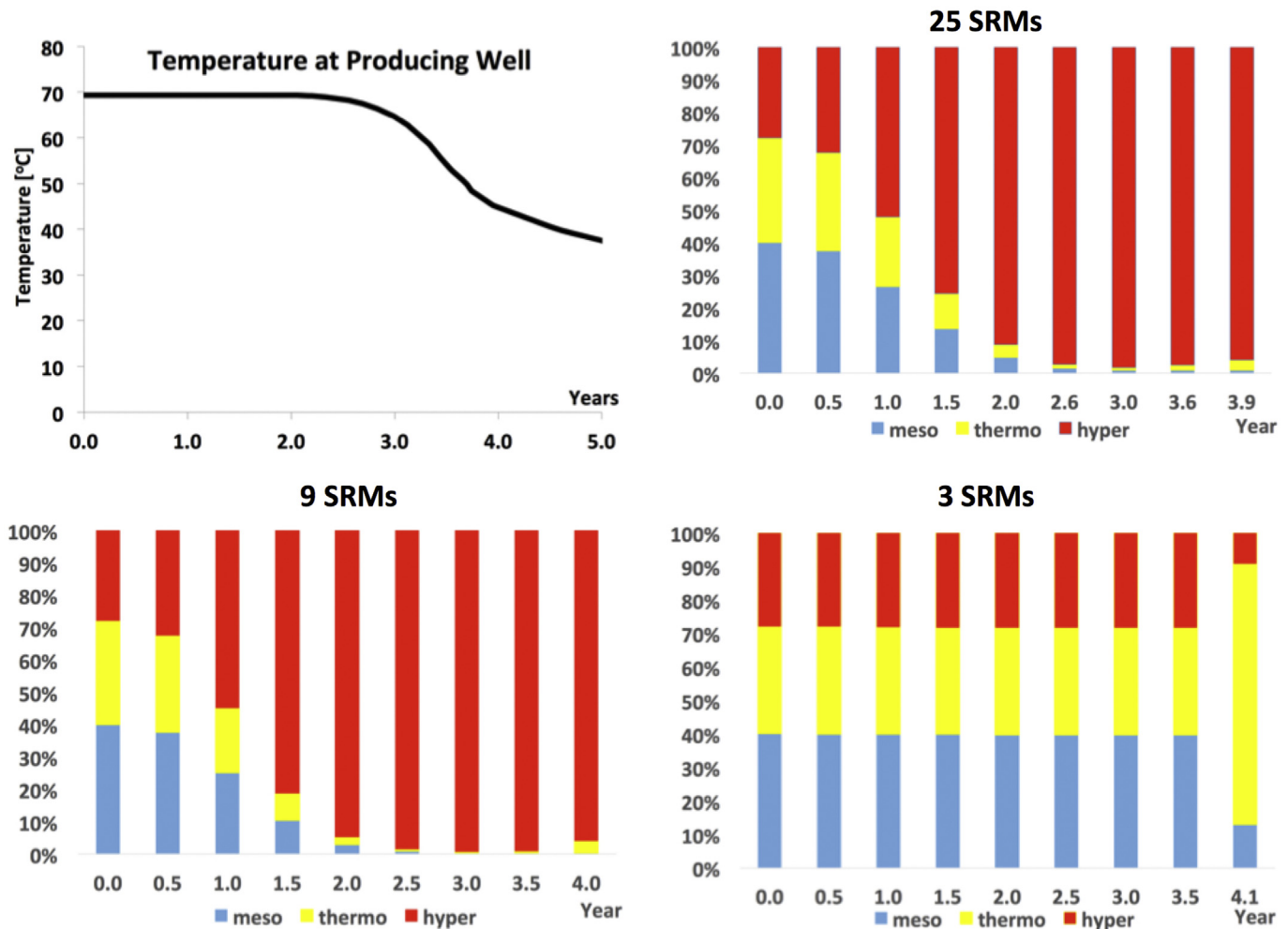


Fig. 11. Comparison of the temporal trends of mesophiles, thermophiles and hyperthermophiles distribution at the producing well between the different scenarios.

## Acknowledgements

This work was funded by the Energy Biosciences Institute.

## Appendix A. Supplementary data

Supplementary data related to this article can be found at <http://dx.doi.org/10.1016/j.ibiod.2017.06.014>.

## References

- Alazard, D., Joseph, M., Battaglia-Brunet, F., Cayol, J.L., Ollivier, B., 2010. *Desulfosporosinus acidiphilus* sp. nov.: a moderately acidophilic sulfate-reducing bacterium isolated from acid mining drainage sediments: new taxa: firmicutes (Class Clostridia, order Clostridiales, Family Peptococcaceae). *Extremophiles* 14, 305–312.
- Andrews, J.H., Harris, R.F., 1986. r- and K- selection and microbial ecology. In: Marshall, K.C. (Ed.), *Advances in Microbial Ecology*. Springer, US, pp. 99–147.
- Burger, E.D., Jenneman, G.E., Carroll, J.J., 2013. On the partitioning of hydrogen sulfide in the oilfield systems. In: *SPE International Symposium on Oilfield Chemistry*.
- Cheng, Y., Hubbard, C.G., Li, Li, Bouskill, N., Conrad, M., Molins, S., Zheng, L., Engelbrekton, A., Coates, J.D., Ajo-Franklin, J., 2016. a reactive transport model of sulfur cycling and isotope fractionation as impacted by nitrate and perchlorate treatments. *Environ. Sci. Technol.* 50 (13), 7010–7018. <http://dx.doi.org/10.1021/acs.est.6b00081>.
- Christensen, B., Torsvik, T., Lien, T., 2012. Immunomagnetically captured thermophilic sulfate-reducing bacteria from North Sea oil field waters. *Appl. Environ. Microbiol.* 58 (4), 1244.
- Corey, A.T., 1954. The Interrelation between Gas and Oil Relative Permeabilities. *Producers Month*, pp. 38–41.
- Dalsgaard, T., Bak, F., 1994. Nitrate reduction in a sulfate-reducing bacterium, *Desulfovibrio-Desulfuricans*, isolated from rice paddy soil sulfide inhibition, kinetics, and regulation. *Appl. Environ. Microbiol.* 60, 291–297.
- Dahle, H., Garshol, F., Madsen, M., Birkeland, N., 2008. Microbial community structure analysis of produced water from a high-temperature North Sea oil-field. *Antonie Leeuwenhoek* 93, 37–49.
- Duan, Z., Sun, R., Liu, R., Zhu, C., 2007. Accurate thermodynamic model for the calculation of H<sub>2</sub>S solubility in pure water and brines. *Energy & Fuels* 21, 2056–2065.
- Farhadinia, M.A., 2008. Development and Implementation of a Multi-Dimensional Reservoir Souring Module in a Chemical Flooding Simulator (UTCHEM). PhD Dissertation. The University of Texas at Austin.
- Follows, M.J., Dutkiewicz, S., Grant, S., Chisholm, S., 2007. Emergent biogeography of microbial communities in a model ocean. *Science* 315, 1843.
- Fukui, M., Takii, S., 1994. Kinetics of sulfate respiration by free-living and particle-associated sulfate-reducing bacteria. *FEMS Microbiol. Ecol.* 13, 241–247.
- Fuller, D.C., Suruda, A.J., 2000. Occupationally related hydrogen sulfide deaths in the United States from 1984 to 1994. *J. Occup. Environ. Med.* 42, 939–942. <http://dx.doi.org/10.1097/00043764-200009000-00019>.
- Gilmour, C.C., Elias, D.A., Kucken, A.M., Brown, S.D., Palumbo, A.V., Schadt, C.W., Wall, J.D., 2011. Sulfate-reducing bacterium *Desulfovibrio desulfuricans* ND132 as a model for understanding bacterial mercury methylation. *Appl. Environ. Microbiol.* 77, 3838–3851.
- German, D.P., Marcelo, K.B., Stone, M.M., Allison, S.D., 2012. The Michaelis-Menten kinetics of soil extracellular enzymes in response to temperature: a cross-latitudinal study. *Glob. Change Biol.* 18, 1468–1479.
- Habicht, K.S., Salling, L., Thamdrup, B., Canfield, D.E., 2005. Effect of low sulfate concentrations on lactate oxidation and isotope fractionation during sulfate reduction by *Archaeoglobus fulgidus* Strain Z. *Appl. Environ. Microbiol.* 71, 3770–3777.
- Haghshenas, M., Sepehrnoori, K., Bryant, S., Farhadinia, M., 2012. Modeling and simulation of nitrate injection for reservoir souring remediation. In: *SPE*

- International Symposium on Oilfield Chemistry.
- Hamilton-Brehm, S.D., Gibson, R.A., Green, S.J., Hopmans, E.C., Schouten, S., van der Meet, M.T., Shields, J.P., Damste, J.S., Elkins, J.G., 2013. Thermodesulfobacterium geofontis sp. nov., a hyperthermophilic, sulfate-reducing bacterium isolated from Obsidian Pool, Yellowstone National Park. *Extremophiles* 17, 251–263.
- Head, I.M., Singleton, I., Milner, M.G., 2003. *Bioremediation; a Critical Review*. Horizon Scientific Press, Wymondham, UK.
- Head, I.M., Gray, N.D., Larter, S.R., 2014. Life in the slow lane; biogeochemistry of biodegraded petroleum containing reservoirs and implications for energy recovery and carbon management. *Front. Microbiol.* 5, 566.
- Herrera, L., Hernandez, J., Ruiz, P., Gantenbein, S., 1991. Desulfovibrio desulfuricans growth kinetics. *Environ. Toxicol. Water Qual.* 6, 225–237.
- Hubbard, C.G., Cheng, Y., Engelbrekston, A., Druhan, J.L., Li, L., Ajo-Franklin, J., Coates, J.D., Conrad, M.E., 2014. Isotopic insights into microbial sulfur cycling in oil reservoirs. *Front. Microbiol.* <http://dx.doi.org/10.3389/fmicb.2014.00480>.
- Holt, R.D., 2009. Bringing the Hutchinsonian niche into the 21<sup>st</sup> century: ecological and evolutionary perspectives. *PNAS* 106, 19659–19665.
- Ingvorsen, K., Jørgensen, B.B., 1984. Kinetics of sulfate uptake by fresh-water and marine species of Desulfovibrio. *Arch. Microbiol.* 39, 61–66.
- Ingvorsen, K., Zehnder, A.J.B., Jørgensen, B.B., 1984. Kinetics of sulfate and acetate uptake by Desulfovibrio postgatei. *Appl. Environ. Microbiol.* 47, 403–408.
- Johns, G.C., Somero, G.N., 2004. Evolutionary convergence in adaptation of proteins to temperature:  $\alpha$ -lactate dehydrogenases of Pacific damselfishes (Chromis spp.). *Mol. Biol. Evol.* 21, 314–320.
- Kelland, M.A., 2009. *Production Chemicals for the Oil and Gas Industry*. CRC Press, Boca Raton, Florida.
- Koch, O., Tschirko, D., Kandeler, E., 2007. Temperature sensitivity of microbial respiration, nitrogen mineralization, and potential soil enzyme activities in organic alpine soils. *Glob. Biogeochem. Cycles* 21, GB4017.
- Kublanov, I.V., Bidjjeva, S.K., Mardanov, A.V., Bonch-Osmolovskaya, E.A., 2009. Desulfurococcus kamchatkensis sp. nov., a novel hyperthermophilic protein-degrading archaeon isolated from a Kamchatka hot spring. *Int. J. Syst. Evol. Microbiol.* 59, 1743–1747.
- Le Roux, X., Bouskill, N.J., Niboyet, A., Barthes, L., Dijkstra, P., Field, C.B., Hungate, Lerondelle, B.A.C., Pommier, T., Tang, J., Terada, A., Tourna, M., Poly, F., 2016. Predicting the responses of soil nitrite-oxidizers to multi-factorial global change: a trait-based approach. *Front. Microbiol.* 7, 628.
- Lien, T., Beeder, J., 1997. *Desulfovibrio vibrioformis* sp. Nov., a sulfate reducer from a water-oil separation system. *Int. J. Syst. Bacteriol.* 47, 1124–1128.
- Lien, T., Madsen, M., Steen, I.H., Gjerdevik, K., 1998. Desulfobulbus rhabdoformis sp. nov. a sulfate reducer from a water-oil separation system. *Int. J. Syst. Bacteriol.* 48, 469–474.
- Litchman, E., Klausmeier, C.A., 2008. Trait-based community ecology of phytoplankton. *Annu. Rev. Ecol. Syst.* 39, 615–639.
- MacArthur, R.H., Wilson, E.O., 1967. *The Theory of Island Biogeography*. Princeton Univ. Press, Princeton, NJ.
- Mori, K., Kim, H., Kakegawa, T., Hanada, S., 2003. A novel lineage of sulfate-reducing microorganisms: thermodesulfobiaceae fam. nov., Thermodesulfobium narugense, gen. nov., sp. nov., a new thermophilic isolate from a hot spring. *Extremophiles* 7, 383–390.
- Moridis, G.J., Kowalsky, M.B., Pruess, K., 2008. TOUGH+HYDRATE v1.0 User's Manual: a Code for the Simulation of System Behavior in Hydrate-bearing Geologic Media. Report LBNL-00149E. Lawrence Berkeley National Laboratory, Berkeley, CA.
- Muyzer, G., Stams, J.M., 2008. The ecology and biotechnology of sulfate-reducing bacteria. *Nat. Rev. Microbiol.* 6, 441–454.
- Nethejaenchen, R., Thauer, R.K., 1984. Growth yields and saturation constants of Desulfovibrio vulgaris in chemostat culture. *Arch. Microbiol.* 137, 236–240.
- Novembre, J.A., 2002. Accounting for background nucleotide composition when measuring codon usage bias. *Mol. Biol. Evol.* 19, 1390–1394.
- Okabe, S., Nielsen, P.H., Characklis, W.G., 1992. Factors affecting microbial sulfate reduction by Desulfovibrio desulfuricans in continuous culture – limiting nutrients and sulfide concentration. *Biotechnol. Bioeng.* 40, 725–734.
- Ommedal, H., Torsvik, T., 2007. Desulfotignum toluenicum sp. nov., a novel toluene-degrading, sulfate-reducing bacterium isolated from an oil-reservoir model column. *Int. J. Syst. Evol. Microbiol.* 57, 2865–2869.
- Orbey, H., Sandler, S.I., 1998. *Modeling Vapor-liquid Equilibria: Cubic Equations of State and Their Mixing Rules*. Cambridge University Press.
- Pallud, C., Van Cappellen, P., 2006. Kinetics of microbial sulfate reduction in estuarine sediments. *Geochim. Cosmochim. Acta* 70, 1148–1162.
- Pruess, K., Battistelli, A., 2002. TMVOC, a Numerical Simulator for Three-phase Non-Isothermal Flows of Multicomponent Hydrocarbon Mixtures in Saturated–unsaturated Heterogeneous Media. Lawrence Berkeley National Laboratory, Berkeley, CA, p. 192.
- Ratkowsky, D., Lowry, R.K., McMeekin, T.A., Stokes, A.N., Chandler, R.E., 1983. Model for bacterial culture growth rate throughout the entire biokinetic temperature range. *J. Bacteriol.* 154, 1222–1226.
- Reynolds, C.S., 2006. *The Ecology of Phytoplankton*. Cambridge Univ. Press, Cambridge, UK, 550 pp.
- Rittman, B.E., McCarty, P.L., 2001. *Environmental Biotechnology: Principles and Applications*. McGraw-Hill, New York.
- Rosnes, J.T., Torsvik, T., Lien, T., 1991. Spore-forming thermophilic sulfate-reducing bacteria isolated from North Sea oil field waters. *Appl. Environ. Microbiol.* 57 (8), 2302.
- Rosso, L., Lobry, J.R., Bajard, S., Flandrois, J.P., 1995. Convenient model to describe the combined effects of temperature and pH on microbial growth. *Appl. Environ. Microbiol.* 62, 610–616.
- Roychoudhury, A.N., Viollier, E., Van Cappellen, P., 1998. A plug flow-through reactor for studying biogeochemical reactions in undisturbed aquatic sediments. *Appl. Geochem* 13, 269–280.
- Savage, K.N., Krumholz, L.R., Gieg, L.M., Parisi, V.A., Sufita, J.M., Allen, J., Philp, R.P., Elshahed, M.S., 2010. Biodegradation of low molecule weight alkanes under mesophilic, sulfate-reducing conditions: metabolic intermediates and community patterns. *FEMS Microbiol. Ecol.* 72, 485–495.
- Semcrude, 2011. *Rose Rock Daily Price Bulletin*. <http://crudeoilpostings.semgrouppcorp.com> (Accessed January 2011).
- So, C.M., Young, L.Y., 1999. Initial reactions in anaerobic alkane degradation by a sulfate reducer, strain AK-01. *Appl. Environ. Microbiol.* 65, 5532–5540.
- Somero, G.N., 2004. Adaptation of enzymes to temperature: searching for basic “strategies”. *Comp. Biochem. Physiol. B* 139, 321–333.
- Sommer, U., 1981. The role of r- and K- selection in the succession of phytoplankton in Lake Constance. *Acta Oecol.* 2, 327–342.
- Sonne-Hansen, J., Westermann, P., Ahning, B.K., 1999. Kinetics of sulfate and hydrogen uptake by the thermophilic sulfate-reducing bacteria Thermodesulfobacterium sp. strain JSP and Thermodesulfobacterium sp. strain R1Ha3. *Appl. Environ. Microbiol.* 65, 1304–1307.
- Statoil, 2015. <http://www.statoil.com/en/OurOperations/TradingProducts/CrudeOil/Crudeoilassays> (Accessed January 2015).
- Steinsbu, B.O., Thorseth, I.H., Nakagawa, S., Inagaki, F., Lever, M.A., Engelen, B., Øvreas, L., Pedersen, R.B., 2010. Archaeoglobus sulfatocalidus sp. nov., a novel thermophilic and facultative lithoautotrophic sulfate-reducer isolated from black rust exposed to hot ridge flank crustal fluids. *Int. J. Syst. Evol. Microbiol.* 60, 2745–2752.
- Stetter, K.O., Huber, R., Blochl, E., Kurr, M., Eden, R.D., Fielder, M., Cash, H., Vance, I., 1993. Hyperthermophilic archaea are thriving in deep North Sea and Alaskan oil reservoirs. *Nature* 365, 743–745.
- Stone, M.M., Weiss, M.S., Goodale, C.L., Adams, M.B., Fernandez, I.J., German, D.P., Allison, S.D., 2012. Temperature sensitivity of soil enzyme kinetics under N-fertilization in two temperate forests. *Glob. Change Biol.* 18, 1173–1184.
- Takai, K., Suzuki, M., Nakagawa, S., Miyazaki, M., Suzuki, Y., Inagaki, F., Horikoshi, K., 2006. Sulfurimonas paralvinellae sp. nov., a novel mesophilic, hydrogen- and sulfur-oxidizing chemolithoautotroph within the Epsilonproteobacteria isolated from a deep-sea hydrothermal vent polychaete nest, reclassification of Thiomicrospira denitrificans as Sulfurimonas denitrificans comb. nov. and emended description of the genus Sulfurimonas. *Int. J. Syst. Evol. Microbiol.* 56, 1725–1733.
- Tarpgaard, I.H., Røy, H., Jørgensen, B.B., 2011. Concurrent low- and high affinity sulfate reduction kinetics in marine sediment. *Geochim. Cosmochim. Acta* 75, 2997–3010.
- Vance, I., Thrasher, D.R., 2005. Reservoir souring mechanisms and prevention. In: Ollivier, B., Magot, M. (Eds.), *Petroleum Microbiology*. ASM Press, Washington DC, pp. 123–142.
- Vieira-Silva, S., Rocha, E.P.C., 2010. The systemic imprint of growth and its uses in ecological (meta)genomics. *PLoS Genet.* 6, e100808. <http://dx.doi.org/10.1371/journal.pgen.100808>.
- Warren, E.A., Smalley, P.G., Howarth, R.J., 1994. Part 4: Compositional Variations of North Sea Formation Waters. Geological Society, London, pp. 119–208. *Memiors*, 15.
- Weinbaur, M.G., Hofle, M.G., 1998. Distribution and life strategies of two bacterial populations in a Eutrophic lake. *Appl. Environ. Microbiol.* 64, 3776–3783.
- Wu, Y., Tang, Y., Tringe, S.G., Simmons, B.A., Singer, S.W., 2014. MaxBin: an automated process to recover individual genomes from metagenomes using an expectation maximized algorithm. *Microbiome* 2, 26.
- Xu, T., Spycher, N., Sonnenthal, E., Zhang, G., Zheng, L., Pruess, K., 2011. TOUGH-REACT Version 2.0: a simulator for subsurface reactive transport under non-isothermal multiphase flow conditions. *Comput. Geosci.* 37 (6), 763–774.
- Youssef, N., Simpson, D.R., Duncan, K.E., McInerney, M.J., Folmsbee, M., Fincher, T., Knapp, R.M., 2007. In situ biosurfactant production by Bacillus strains injected into a limestone petroleum reservoir. *Appl. Environ. Microbiol.* 73, 1239–1247.
- Youssef, N., Elshahed, M.S., McInerney, M.J., 2009. Microbial processes in oil fields: culprits, problems, and opportunities. In: Laskin, A.I., Sariaslani, S., Gadd, G.M. (Eds.), *Advances in Applied Microbiology*, vol. 66. Academic Press, Burlington, pp. 141–251.
- Zeldovich, K.B., Berezovsky, I.N., Shakhnovich, E.I., 2007. Protein and DNA sequence determinants of thermophilic adaptation. *PLoS Comput. Biol.* <http://dx.doi.org/10.1371/journal.pcbi.0030005>.
- Zheng, L., Spycher, N., Birkholzer, J., Xu, T., Apps, J., Kharaka, Y., 2013. On modeling the potential impacts of CO<sub>2</sub> sequestration on shallow groundwater: transport of organics and co-injected H<sub>2</sub>S by supercritical CO<sub>2</sub> to shallow aquifers. *Int. J. Greenh. Gas Control* 14 (0), 113–127.
- Zhou, J., He, Q., Hemme, C.L., Mukhopadhyay, A., Hillesland, K., Zhou, A., He, Z., Van Nostrand, J.D., Hazen, T.C., Stahl, D.A., Wall, J.D., Arkin, A.P., 2011. How sulfate-reducing microorganisms cope with stress: lessons from systems biology. *Nat. Rev. Micro* 9, 452–466.